



HAL
open science

Experimental study of lean premixed turbulent combustion

Benoît Taupin, David Vauchelles, Gilles Cabot, Abdelkrim Boukhalfa

► **To cite this version:**

Benoît Taupin, David Vauchelles, Gilles Cabot, Abdelkrim Boukhalfa. Experimental study of lean premixed turbulent combustion. 11th International Symposium on Applications of Laser, 2002, Lisbonne, Portugal. hal-02014967

HAL Id: hal-02014967

<https://hal.science/hal-02014967>

Submitted on 11 Feb 2019

HAL is a multi-disciplinary open access archive for the deposit and dissemination of scientific research documents, whether they are published or not. The documents may come from teaching and research institutions in France or abroad, or from public or private research centers.

L'archive ouverte pluridisciplinaire **HAL**, est destinée au dépôt et à la diffusion de documents scientifiques de niveau recherche, publiés ou non, émanant des établissements d'enseignement et de recherche français ou étrangers, des laboratoires publics ou privés.

Experimental study of lean premixed turbulent combustion

Benoît TAUPIN , David VAUCHELLES, Gilles CABOT and Abdelkrim BOUKHALFA

CORIA UMR CNRS 6614

INSA avenue de l'université BP8 76801 Saint Etienne Du Rouvray (France)

Abstract

The purpose of this experimental study is to identify the factors that give rise to combustion instability in case of lean premixed combustion. The studied experimental device is gas turbine combustor, where the flame is stabilized in the dump combustor with a swirling and bluff-body injector. This combustor is optically accessible. A parametrical study has been conducted in the way to provide information on the effect of the equivalence ratio, ϕ , while the mean inlet velocity remains constant. LDV and OH^* chemiluminescence measurements were performed in the reacting flows for a 50° swirler and for different equivalence ratio conditions. LDV measurements show that two distinct recirculations zones appears in the resulting flow. One is formed in the corner due to the sudden-expansion, while the other one is due to the swirling motion of the incoming flow. In order to obtain the 2D mean reaction location, an Abel deconvolution algorithm is applied to the average of 200 OH^* chemiluminescence images. It allows to enhance the following relationships: as the premixing becomes leaner, the flame takes different locations in the flow. For $\phi > 0.7$, the flame is in a steady state, anchored near the bluff-body between the two recirculation zones. For $0.7 > \phi > 0.65$, an extension of reaction zone occurs in the corner recirculation zone and downstream near the quartz tube. For $0.65 > \phi > 0.6$, the flame becomes unsteady and an oscillation of the OH^* emission intensity occurs with the same frequency as measured by dynamic pressure in the combustion chamber (≈ 16 Hz). For $\phi = 0.57$, the flame becomes stable again without any reaction in the corner recirculation zone. When ϕ is more reduced ($\phi < 0.57$), the blow-out occurs. In order to characterize the unsteady state, CH^* visualization is realized by triggering acquisition with the temporal signal of pressure. Results shows a periodic behavior of flame position and combustion intensity. The analysis of all results shows a coupling between the cyclic phenomenon of vortex shedding and fluctuations in gas supply inducing a cyclic equivalence ratio at the inlet.

1. INTRODUCTION

One way to reduce the pollutant emissions while maintaining combustion efficiency in gas turbine engines is the LPP concept: an homogeneous lean fuel-air mixture is delivered into the primary zone, and combustion occurs at lower temperatures because the fuel burns at lean equivalence ratios. Unfortunately, it turns out that this modus operandi often leads to combustion instabilities, and therefore engine components could undergo structural damages (Lefebvre, 1999). Different factors are involved to explain the occurrence of instability at lean condition. One of these factors is the presence of resonance phenomena between the acoustic mode of the couple flame and combustion chamber (Santorro et al., 1998). This phenomenon occurs when the inlet fuel supply is not choked because oscillations of the combustion chamber go upstream in gas supply and induce some fluctuations on the inlet equivalence ratio (Nguyen, 2001), (Lieuwen et al., 1998). Many studies investigate an active control of these instabilities, by localizing the region where the pressure chamber is in phase with heat release. Then a damping process of the instability can be applied, either by introducing secondary injection in these zones (Santavicca et al., 2000), or by using an acoustic stimulation (Pashcherett et al., 2000). A second factor which drives the lean combustion instability is the aerodynamic instability of the swirling flow at high Reynolds number which leads to vortex breakdown. This vortex shedding in the flow exerts an influence on the flame stability (Syred et al., 1984) and can induce local extinction, particularly for low equivalence ratio. When the coherent structure crosses a region where the flame is not well anchored, the increase of stretching can induce extinction (Bradley et al., 1998).

The purpose of the present experimental study of lean premixed combustion in swirling flows is to study the factors which govern the lean-burn instability. Our experimental setup uses a premixed air / natural gas swirl stabilized burner. This kind of injector is often used to stabilize flames in lean premixing condition. The swirl induces a reverse flow on the chamber axis, which drags hot combustion products towards the injector and stabilize the flame. Due to the confinement, another recirculation zone appears in the corner of the combustion chamber, near the injection plane. A low frequency instability of this corner recirculation occurs when the equivalence ratio is decreased.

2. EXPERIMENTAL SETUP

The experimental configuration uses a swirler and a bluff-body in a sudden-expansion dump combustor which made of a quartz tube for an optical access. The swirler has six curved vanes with an 50° angle with the axial direction, which yields to a swirl number ($Sn = 0.88$) based on the swirler geometry. In order to allow natural gas injection, and a complete premixing of natural gas and air, ten holes are located at (30 mm) behind the exit of the injector. The confinement ratio of the burner is $A_c / A_i = 24.6$, where A_c is the combustor section and A_i is the injection section. The Bluff Body is located flush with the dump plane of the combustor section.

In a first study, a free exhaust burner is used, in atmospheric pressure condition (see Fig. 1-a). LDV and OH* chemiluminescence measurements were performed. The combustion chamber is composed of a 80 mm diameter and 200 mm long quartz tube to allow optical access. The LDV measurement device is a two color, dual beam TSI system. Axial and radial velocity components are measured using respectively the green and the blue lines from a 6 W Argon Ion laser. Directional ambiguity for the components is avoided by a frequency shifting. The LDV signal is processed by an IFA 750 Digital Burst Correlator. The swirling incoming air jet was seeded with zirconium oxide (mean diameter $\sim 2 \mu\text{m}$) introduced in the flow by a rotative brush seeder. For OH* emission measurements an intensified CCD camera was used (Princeton IMAX 512 THM, 16 bytes, 512 pixels^2 , field of view 8.7 cm^2). OH* emission was filtered at 308 nm with an interferential filters.

For higher pressure measurements, a restricted exhaust burner is used and is presented in Fig.1-b. The total chamber length is 370 mm. A conical converging nozzle is placed at the chamber exit to allow pressure modification. Dilution air flow is injected at 230 mm downstream air/fuel injection, in order to cool the quartz tube and to dilute the hot combustion product. To limit the strain of pressure and temperature on the quartz tube, it was placed in a square box equipped with three wide windows for optical access. Three mass flow controllers are used to fix the cooling dilution air, the combustion air and the natural gas flow rates, full scale are respectively: "250 Nm^3/h for air and 25 Nm^3/h for the gas". This experimental set-up allows a parametrical investigation of equivalence ratio (ϕ) and pressure chamber (P) influences. Pressure measurements are obtained by a dynamic pressure sensor with a 45 kHz response (Kistler: 7061B), which was calibrated between 0 and 5 bars. This sensor is coupled to a charge amplifier with a 70 kHz cut frequency. The sensor is fixed at the end of the combustion chamber. This sensor was submitted to the action of both combustion air and cooling dilution air; however the action of this secondary airflow has not shown an important effect during acquisition. Phase-lock images of CH* emission were obtained with an intensified CCD camera (LaVision: Flamstar2, 14 bytes, $384 \times 576 \text{ pixels}^2$, field of view $7.6 \times 10 \text{ cm}^2$). CH* emission was filtered with two colored filters, the first one is 180 nm band pass centered on 410 nm and the other one is high pass with a cut frequency at 390 nm. During

these acquisitions, images were triggered with the pressure signal filtered with a 100 Hz low band-pass filter. This selective filter ensure a phase locking on the lowest frequency observed in the flame (<20 Hz).

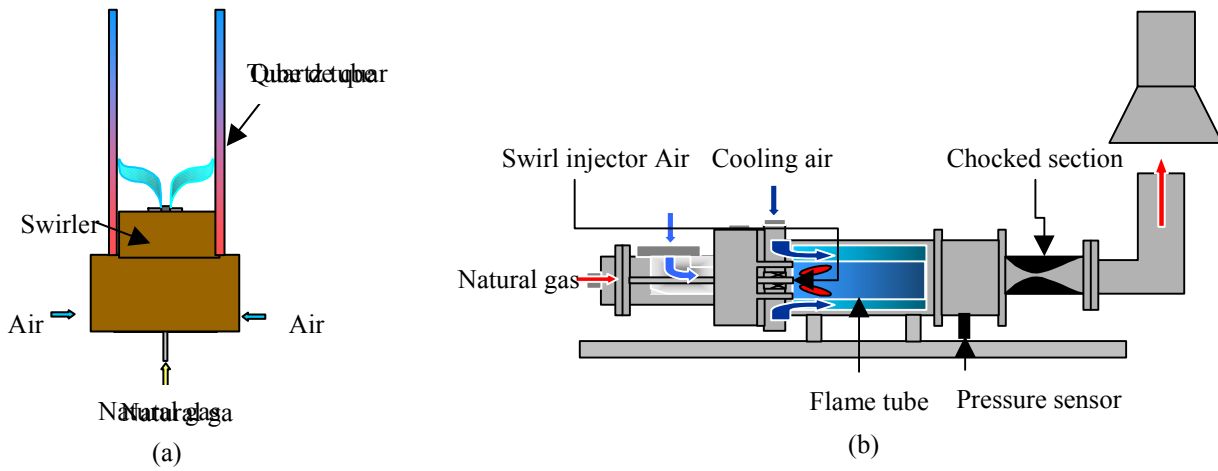


Fig.1.a-b. (a) Atmospheric pressure burner , (b) High pressure facility

3. RESULT AND DISCUSSION

3.A/ OH* chemiluminescence measurements

The recorded emissions are principally from OH*, COO* and CH* (see Fig.2). It is well known (Samaniego et al., 1995) that OH*($\lambda = 308 \text{ nm}$) and CH*($\lambda = 431 \text{ nm}$) are very good indicators of the reaction zone. In our case, the highest signal comes from OH*. But the OH* UV wavelength are partially absorbed by the optical device of UV lenses and therefore longer exposition time is required. Due to this reason, measurements in phase locked mode were made with the CH* radical signal.

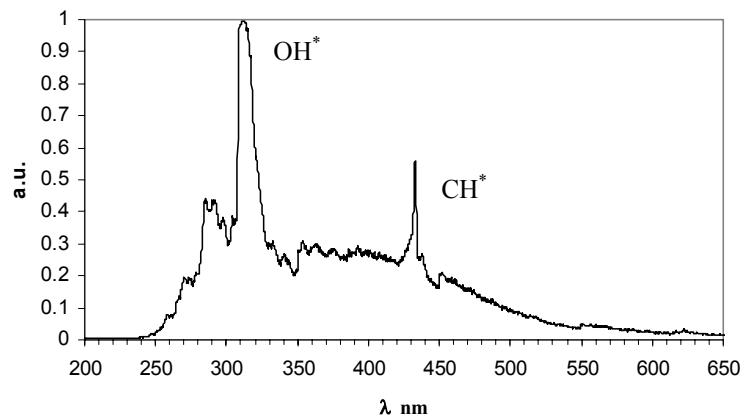


Fig. 2 Spectral emission of the lean premixed swirl stabilized flame $\phi = 0.7$

For an equivalence ratio higher than 0.7, a stable flame well anchored on the bluff body edge is observed. When the mixture equivalence ratio decreases, the flame becomes unstable with a maximum of fluctuations for 0.6 value of the equivalence ratio. For higher equivalence ratio, the flame becomes stable again with a different shape. In figure 3, averages of 200 OH^* images are reported for five different conditions of equivalence ratio. The maximum contrast of each image increases the visibility of the phenomenon. In reality, the signal is five time less for $\phi = 0.57$ than for $\phi = 0.7$. These averaged images are a good indicator of the mean flame position. For example, the flame extends downstream when the equivalence ratio decreases. For stable cases ($\phi = 0.7$ and $\phi = 0.57$) no reaction occurs in the corner of the combustion chamber. For $0.7 < \phi < 0.57$, the flame moves inside the corner. More precise information appears when Abel deconvolution algorithm is applied on the right half part of the images (Fig. 4). For rich premixed ($\phi > 0.7$), the flame is in a steady state well anchored on the edge of the bluff-body, it is localized between the two recirculation zones IRZ (Inner Recirculation Zone) and CRZ (Corner Recirculation zone). These recirculation zones, which are obtained by LDV measurements, are represented by the white arrow on the first OH^* averaged image. For ($0.7 < \phi < 0.6$) the reaction zone extends both in the CRZ and downstream near the quartz tube. For ($\phi = 0.6$), the flame presents a strong instability at a frequency about 16 Hz, extinction and ignitions occur successively in the CRZ. Further decrease of the equivalence ratio leads to an extinction of the reaction zone in the CRZ.

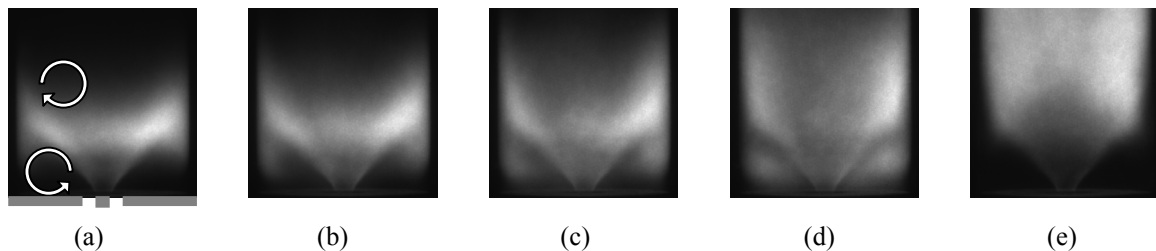


Fig.3.a-e. Averaged images of OH^* (a) $\phi=0.7$, (b) $\phi=0.65$, (c) $\phi=0.63$, (d) $\phi=0.6$, (e) $\phi=0.57$

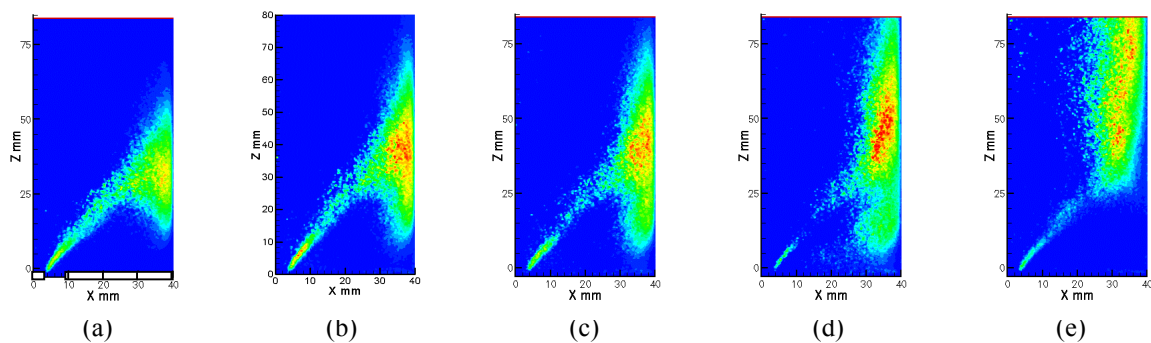


Fig.4.a-e. Corresponding Abel deconvolution (a) $\phi=0.7$, (b) $\phi=0.65$, (c) $\phi=0.63$, (d) $\phi=0.6$, (e) $\phi=0.57$

3. B/ LDV measurements

Figure 5 shows the averaged velocity field for three different values of the equivalence ratio. It can be noticed that no correction is applied to take into account optical aberration due to the cylindrical quartz tube. As a consequence, a small uncertainty can exist for measurement points located near the tube wall. For these

positions, a loss of burst signal is due to the fact that the overlapping between collection volume and measurement volume is not complete. Furthermore, some difficulties are encountered for flow seeding due to the centrifugation of particles by the swirl, which leads to a dirtying of the tube and generates a measurement bias in the external mixing layer of the swirling jet. On the averaged velocity map, we can distinguish the presence of two recirculation zones, the first one called IRZ is located on the axis, and is due to swirling incoming flows. The second one called CRZ, is due to the step between the injector and the combustor.

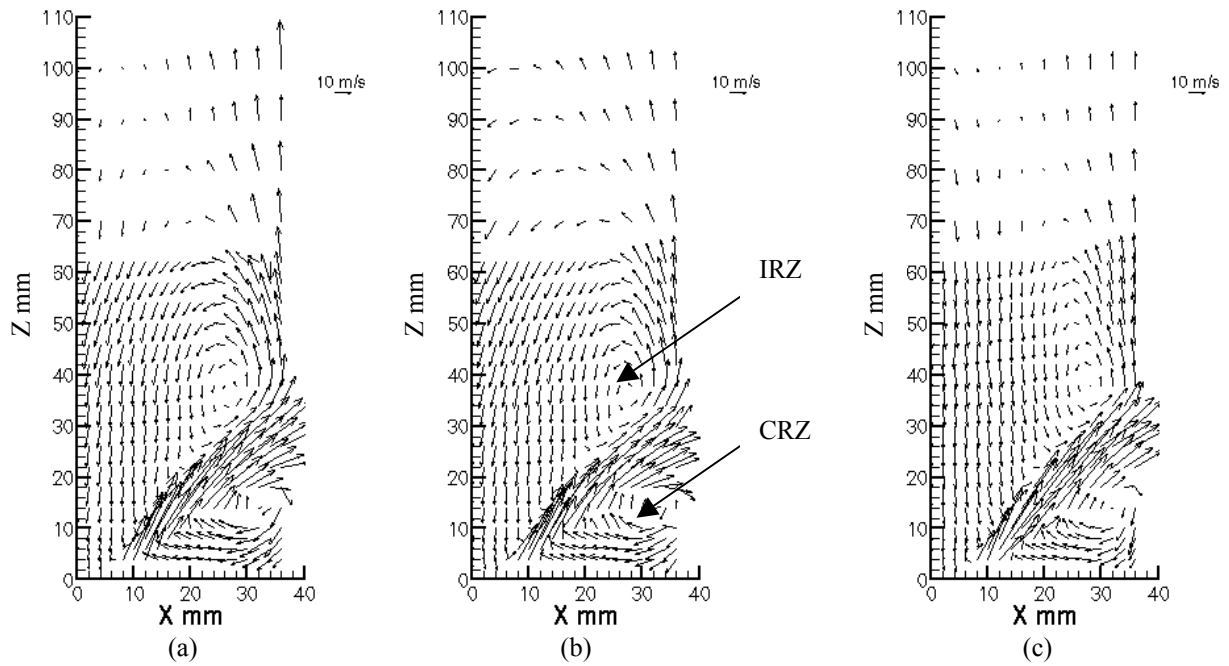


Fig.5 Mean axial-radial velocity map for -a $\phi = 0.65$, -b $\phi = 0.6$, -c $\phi = 0.57$.

There is not a big difference between the mean velocity patterns for the three different investigated conditions ($\phi = 0.65$, $\phi = 0.6$, $\phi = 0.57$). The r.m.s. of the axial velocity (Fig 6 -a, -b) shows an evolution between the unsteady state ($\phi = 0.6$) and the steady state ($\phi = 0.57$). The r.m.s. values is high in the mean reaction zone location and is weak elsewhere. In the unsteady case, the r.m.s value is roughly 20 m/s in the CRZ, which is very high compared to the 30 m/s inlet velocity (black circle on the map). We can make the following hypothesis which is in good agreement with OH^* images: there is a succession of burned and unburned pockets of gas in the CRZ. For $\phi = 0.57$, these high r.m.s. values disappear from the CRZ, as also observed on OH^* image (stable flame with no reaction in the CRZ). It looks possible that the CRZ would drive and amplify the instability. The overlapping of the velocity map with the Abel deconvolution OH^* images gives us information about the mean position of the reaction in the velocity field (Fig.7). The reaction zone is initiated near the injector exit on the inner shear layer of the swirling jet, at this location the axial velocity is close to zero. We can see on (Fig.4) that the flame becomes weak in this shear region when the equivalence ratio is decreased. High shear strain combined with lean conditions and velocity fluctuations might provoke extinctions. As a result, the signal in this zone becomes weaker than in other regions when the equivalence ratio is decreased.

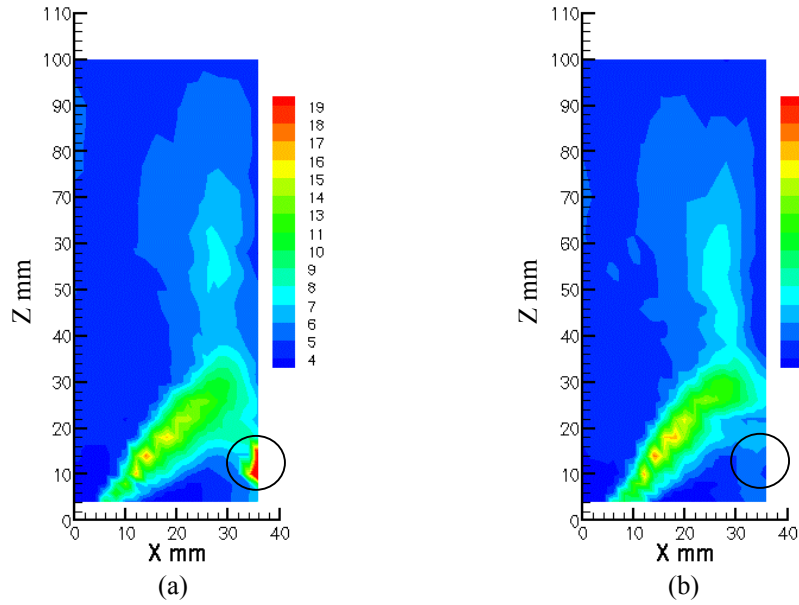


Fig.6 a-b Mean axial velocity fluctuation map (a) $\phi = 0.6$, (b) $\phi = 0.57$

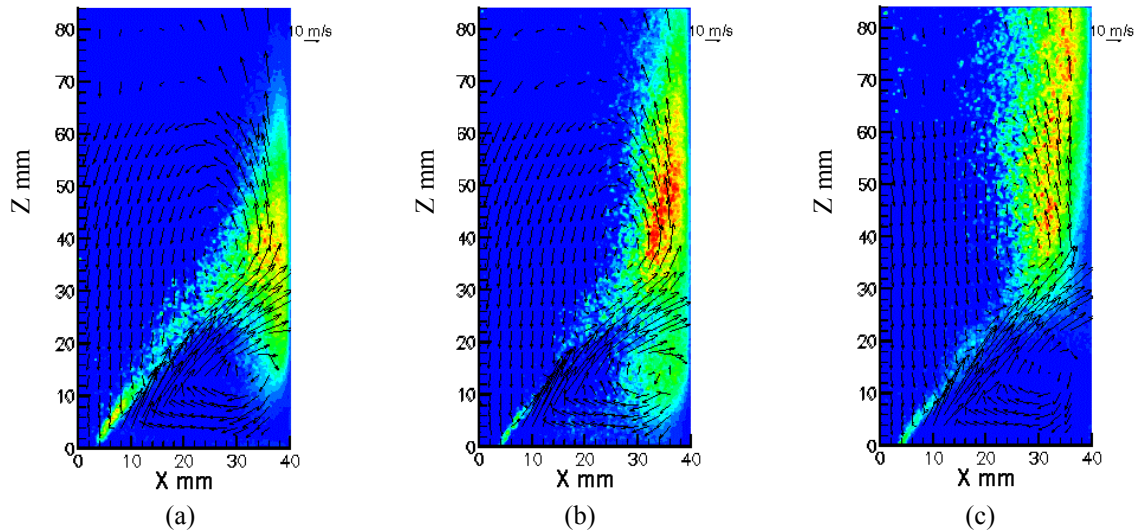


Fig.7 a-c Overlapping of the axial-radial velocity map with the Abel deconvolution for (a) $\phi = 0.65$, (b) $\phi = 0.6$, (c) $\phi = 0.57$

3. C/ Conditioned CH^* chemiluminescence images on combustion chamber pressure

CH^* emissions measurements are performed in the restricted exhaust burner (Fig.1-b), at atmospheric pressure and for the unsteady state $\phi \sim 0.63$. Which is the limit of the blow out condition.

In this case ($\phi \sim 0.63$), a high level of pressure fluctuation ($P_{\text{rms}} = 0.15$ bar) is detected inside the combustion chamber. The oscillation frequency (16 Hz, cf. Figure 6-b) is too low to be an acoustic mode of the combustion chamber.

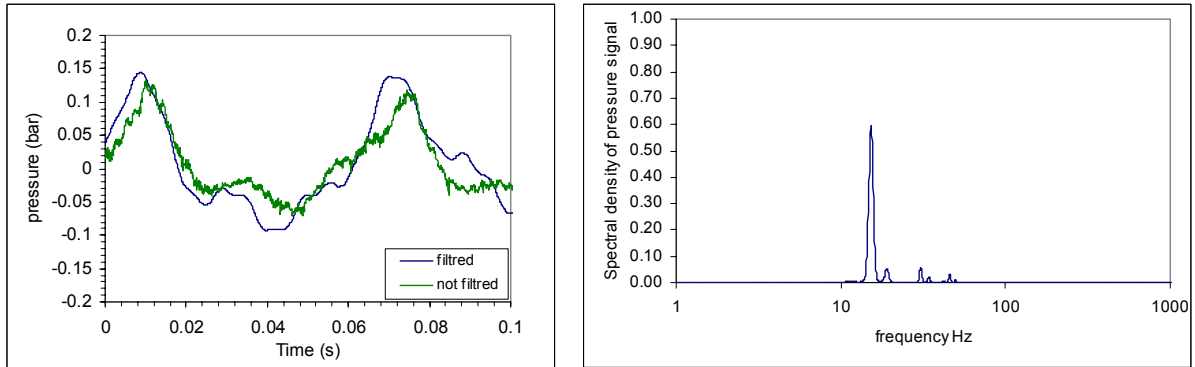


Fig.8 a-b (a) pressure chamber signal, (b) spectral density of pressure signal

In order to obtain information on the flame evolution during the pressure cycle, phase pressure measurements of CH^* are performed. Instantaneous pressure signal is filtered as shown in Fig. 8-a, and CH^* visualization is triggered with the filtered signal. Averaged images are obtained on 200 instantaneous images, and the process is repeated for different values of the phase in the pressure cycle.

Resulting images are reported in figure 9, a phase of 0° correspond to the maximum value of the pressure cycle. The CH^* intensity follows the pressure level : the maximum and the minimum are obtained respectively for 0° and 180° phase angles (maximum and minimum pressure). Minimum intensity is five times weaker than maximum intensity.

The observed flame shape for 0° is similar to the stable flame presented on figure 3-a for the free exhaust burner at $\phi = 0.7$. For phase angle between 100° to 150° , the flame propagates in the CRZ and downstream near the wall of the quartz tube. For 180° phase angle, the flame shape became similar to the free exhaust burner mean flame at $\phi = 0.57$, the intensity on the bottom of the flame is very low. At 240° phase angle, the flame is quite lifted.

In conclusion, the flame shape and intensity obtained for 0° and 180° phase angles look similar to flame shapes and intensity in the free exhaust burner at respectively $\phi = 0.7$ and $\phi = 0.57$, which are the two stable cases previously described. The flame in the restricted exhaust burner behaves like if an oscillation of inlet mixture equivalence ratio occurs. Additional pressure measurements in the inlet gas supply confirm the presence of pressure oscillations, which might induce oscillations of gas flow rate.

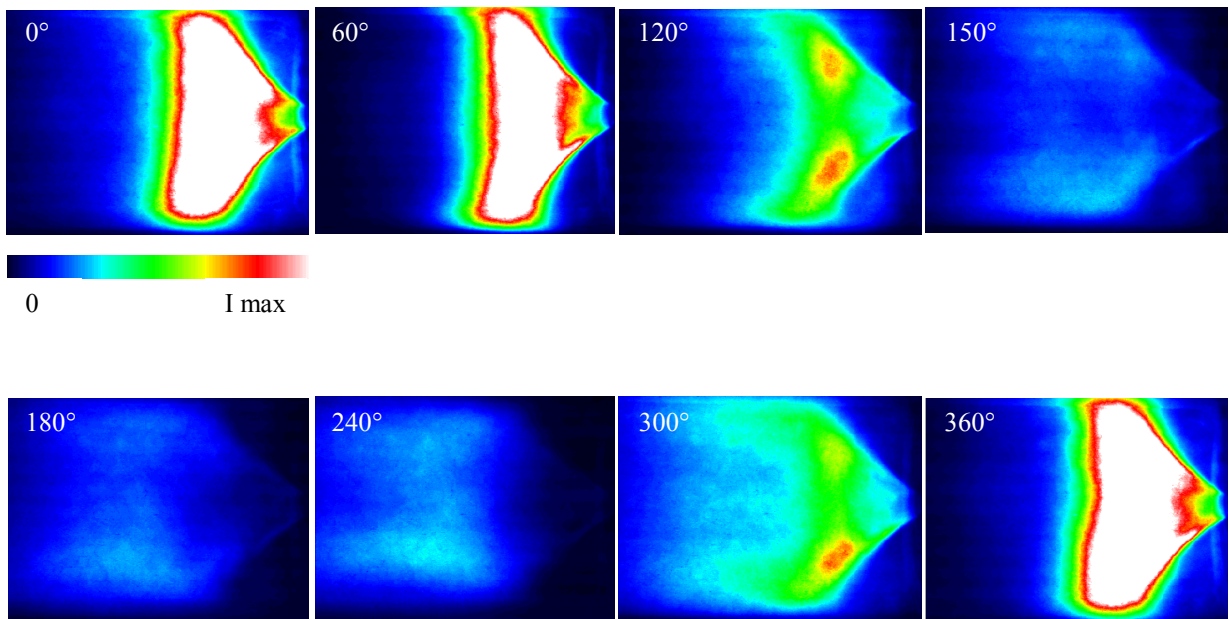


Fig.9. Phase-averaged of CH^* chemiluminescence images during one period of unstable combustion

4 Conclusion

A confined swirl stabilized burner has been studied for low equivalence ratio of premixed methane / air. Due to dump combustor geometry and to swirling injection, two recirculation zones exist inside the combustion chamber, namely the CRZ in the corner and the IRZ on the chamber axis. This flow configuration in the case of a free exhaust at the chamber exit is the same as in the case of a restricted exhaust. Low frequency instabilities have been detected for both exhaust cases. When the burner exit is free, two different steady states are obtained for two different values of the equivalence ratio, namely $\phi > 0.7$ and $\phi = 0.57$. Between these two values, flame is unstable. When the burner exit is restricted, steady state exists only for $\phi > 0.7$. For lower equivalence ratios, pressure oscillations appear at 16 Hz frequency. Measurements were performed for $\phi = 0.63$, which is the leanest case before extinction. Phase averaged images of CH^* show that the flame shape oscillates between the two steady states obtained in the free exhaust burner. These oscillations are probably initiated by natural fluctuations of the annular swirling jet, which can induce periodic vortex shedding. OH^* and LDV measurements show that the reaction zone in the inner shear zone is considerably reduced when equivalence ratio is decreased, while axial velocity fluctuations keep a high value. Instability can be amplified by local extinction in the lean mixture case, or by periodic extinction if periodic vortex shedding is involved. The reignition can occur by the downstream reaction zone who recirculate in the CRZ. When the burner exit is restricted, heat release fluctuations induce pressure fluctuations and lead to a variation of inlet mixture equivalence ratio. As a consequence, restricting exit of combustion chamber could induce a growth of unsteady phenomenon. In order to understand more precisely the coupling of the different phenomenon, further pressure conditioned measurements of velocity field, inlet equivalence ratio, and reaction zone visualization will be performed, respectively with a PIV (particle Image Velocimeter) system, acetone/LIF, and CH^* emission.

Acknowledgement :

The authors would gratefully acknowledge Dr Beduneau for his help and discussions and Dr Honore for his assistance on phase averaged flame pictures and Abel deconvolution processing.

REFERENCES

1. Bradley, D., Gaskell, P.H., Gu, X.J., Lawes, M. and Scott, M.J. (1998), Premixed turbulent flame instability and NO formation in a lean-burn swirl burner, *Comb. and Flame*, 115, pp 515-538.
2. Broda, J.C., Seo, S., Santoro, R.J., Shirhattikar, G. and Yang, V. (1998), An experimental study of combustion dynamics of a premixed swirl injector, *Proc. 27th Intl. Symp. On Combustion*, pp.1849-1856.
3. Lee, J.G., Kim, K. and Santavicca, D.A (2000), Effect of injection location on the effectiveness of an active control system using secondary fuel injection, *Proc. 28th Intl. Symp. On Combustion*, pp.739-746.
4. Lefebvre A. H.(1999), *Gas Turbine Combustion*, 2nd Ed., Taylor and Francis, ISBN: 1-56032-673-5.
5. Lieuwen, T. and Zinn, B.T.(1998), The role of equivalence ratio oscillations in driving combustion instabilities in low NO_x gas turbines, *27th Intl. Symp. On Combustion*, pp.1809-1816.
6. Nguyen, Q.(2001), Measurements of ratio fluctuations in a lean premixed prevaporized (LPP) combustor and its correlation to combustion instability, Submitted to *J. of Engr. for Gas Turbines and Power* May 14.
7. Paschereit, C.O., Gutmark, E. and Weisenstein, W.(2000), Excitation of thermoacoustic instabilities by interaction of acoustics and unstable swirling flow, *AIAA Journal*, 38, (6), pp 1025-1034.
8. Samaniego, J.M., Egolfopoulos, F. M. and Bowman (1995), CO_2^* chemiluminescence in premixed flames *Combust. Sci. and Tech.*, 109, pp.183-203.
9. Samaniego, J.M., Yip, B., Poinso, T. and Candel (1993), CO_2^* Low-frequency combustion instability mechanisms in aside-dump combustor, *Comb. and Flame*, 94, pp.363-380.
10. Syred, N., Lilley, D.G. and Gupta, A.K. (1984), *Swirl Flows*, 1st Ed, Abacus Press, ISBN : 0-85626-175-0.